Proceedings IRF2018: 6th International Conference Integrity-Reliability-Failure
Lisbon/Portugal 22-26 July 2018. Editors J.F. Silva Gomes and S.A. Meguid
Publ. INEGI/FEUP (2018); ISBN: 978-989-20-8313-1

PAPER REF: 7285

STRUCTURAL CONTROL OF A SDOF FRAME WITH NON-LINEAR HYSTERETIC BEHAVIOR USING A TUNED MASS DAMPER

Pedro L.P. Folhento[1(*)], Manuel T. Braz-César[2], António M.V. Paula[2], Rui C. Barros[3]
[1]Master in Civil Engineering, Polytechnic Institute of Bragança
[2]Department of Applied Mechanics, Polytechnic Institute of Bragança
[3]Department of Civil Engineering, Faculty of Engineering of the University of Porto
[(*)]*Email:* pedro.lp.folhento@gmail.com

ABSTRACT

This paper presents a parametric study on the control parameters of a Tuned Mass Damper (TMD) to reduce the seismic response of a simple framed structure with non-linear hysteretic behavior. A numerical model was implemented in MATLAB/Simulink to obtain the structural response and evaluate the contribution of each control parameter to the system. Based on the results, it can be concluded that the appropriate definition of some control parameters are crucial to reach rapidly and consistently the optimal TMD performance.

Keywords: structural control, passive systems, tuned mass damper (TMD).

INTRODUCTION

Tuned mass dampers (TMDs) are common passive control devices for full-scale civil engineering applications such as tall buildings, bridges, towers and other slender structures. The design procedure requires the definition of some control parameters selected in accordance with the properties of the system that is being controlled. The main purpose is to reduce the motion (usually displacement and/or acceleration amplitude) of a structural system under wind or earthquake excitation. Although typical structural design is based on linear elastic analyses, actual civil structures are indeed non-linear and complex systems that are usually linearized to simplify the design procedure. Furthermore, non-structural components are neglected in this stage contributing to the simplification of the real structural behavior.

The implementation of passive control systems assuming an elastic response is required to ensure an elastic structural performance during large earthquake events. However, real structural systems present some type of non-linearities that is not taken into consideration in the design process. Since tuning the control parameters of a TMD requires knowledge about the structure properties, those non-linearities can compromise the overall performance of the control system (Paredes, 2008).

This paper presents a numerical analysis to investigate the influence of some control parameters of a TMD in reducing the response of a non-linear system. In this case the TMD is used as a passive harmonic absorber to control the lateral displacement of a single degree-of-freedom (SDOF) structure under seismic excitation. A parametric study is carried out to highlight the importance of each parameter in the system response. For instance, the mass ratio (i.e., the ratio between the mass of the TMD and the mass of the structure) is of particular importance to achieve the optimal controlled response. Hence, the effect of this

parameter is used to assess the performance of the TMD in the presence of structural components with inelastic behavior.

NUMERICAL MODEL

The numerical model of the controlled structure under the seismic excitation is shown in Figure 1. It shows a two degree-of-freedom (2-DOFs) system representing a single-story framed structure, m_1, equipped with a TMD, m_2. The main structure is connected to the exterior by a spring of stiffness k_1, and by a damping constant c_1. In like manner, the TMD is connected to the main structure by a spring of stiffness k_2, and by a damping constant c_2.

A Simulink model was implemented based on the properties of the structural system. It was considered in this study the following parameters: mass of the structure $m_1 = 5000kg$; the period $T = 1.0s$ and the structural damping coefficient $\xi = 0.05$.

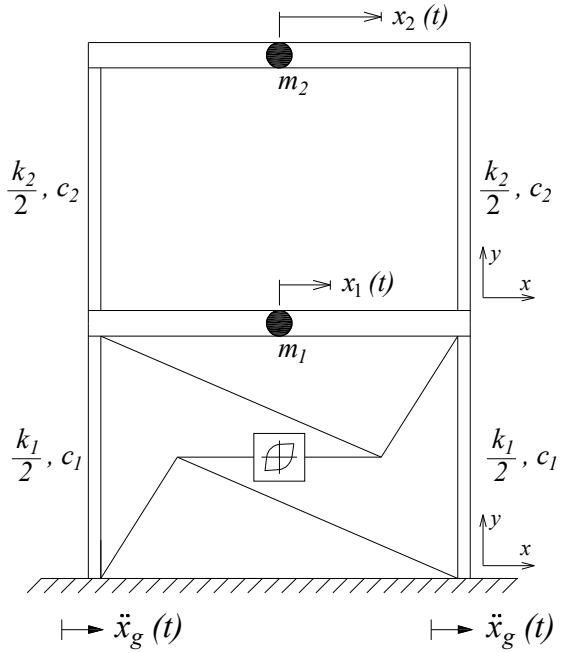

Fig. 1 - Schematic representation of the two DOFs structural system.

The Macro-Simulink numerical model is based on a smooth hysteretic model originally suggested by Bouc. The Macro-Simulink model used in this study was modified and adapted from Mousavi, *et al*, 2015 1967 (Wen, 1976, Baber and Noori, 1985, Casciati, 1989, Reinhorn *et al.*, 1995, Sivaselvan and Reinhorn, 2000, Braz-César *et al*. 2013).

To verify the influence of an infill wall in the performance of a TMD, it was considered three cases of hysteretic behavior of the non-structural wall. The first case is a plain hysteretic behavior without any degradation. In the second case of hysteretic behavior only the stiffness degradation will be considered. The third case, in addition to the stiffness degradation, it will be considered the strength degradation of the non-structural wall.

In each case of hysteretic behavior, the value of the mass ratio was changed giving $\mu = 0.05$, $\mu = 0.10$, $\mu = 0.15$ and $\mu = 0.20$, to assess the performance of the TMD in the presence of structural components with inelastic behavior, looking for the optimal controlled response.

Table 1 - Considered hysteretic parameters to simulate deferent frame behaviors (in all cases, $\boldsymbol{k_0 = 3\ \mathrm{MN/m}}$, $\boldsymbol{P_{fy} = 30\ \mathrm{kN}}$, $\boldsymbol{N = 5}$, $\boldsymbol{a = 0.03}$, $\boldsymbol{\eta = 1}$).

Case	Hysteretic behavior	α	β_1	β_2
0	Plain	50	0	0
I	Stiffness degradation	1	0	0
II	Stiffness and strength degradation	1	0.3	0.3

Mousavi *et al*., 2015.

This study will be carried out using two different acceleration signals (Folhento, 2017). One represents a harmonic generic signal composed by five sections with different and growing acceleration as can be seen in Figure 2 and its corresponding function in Equation 1. The second proposed signal, represented in Figure 3, is the ground acceleration of the well-known El Centro earthquake, occurred in southeastern California on May 18, 1940.

$$\text{Generic Signal} \rightarrow \begin{cases} \sin(2\pi t), & \text{for} \quad 0s \le t < 4s \\ \frac{3}{2}\sin(2\pi t), & \text{for} \quad 4s \le t < 8s \\ 2\sin(2\pi t), & \text{for} \quad 8s \le t < 12s \\ 3\sin(2\pi t), & \text{for} \quad 12s \le t < 16s \\ 0, & \text{for} \quad t \ge 16s \end{cases} \tag{1}$$

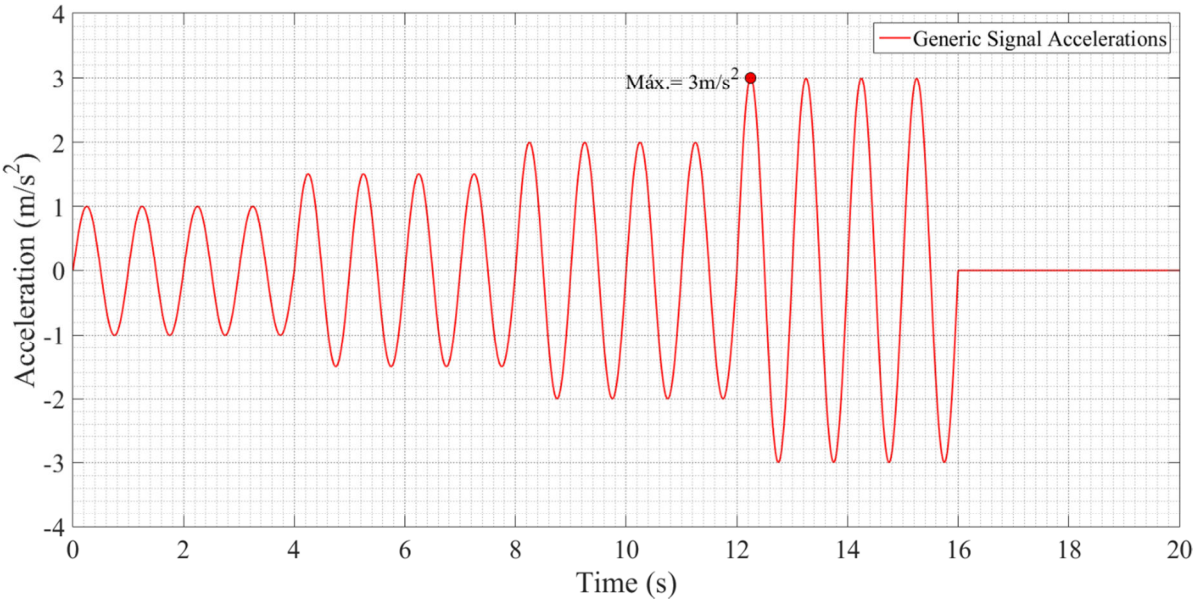

Fig. 2- Generic harmonic signal accelerations.

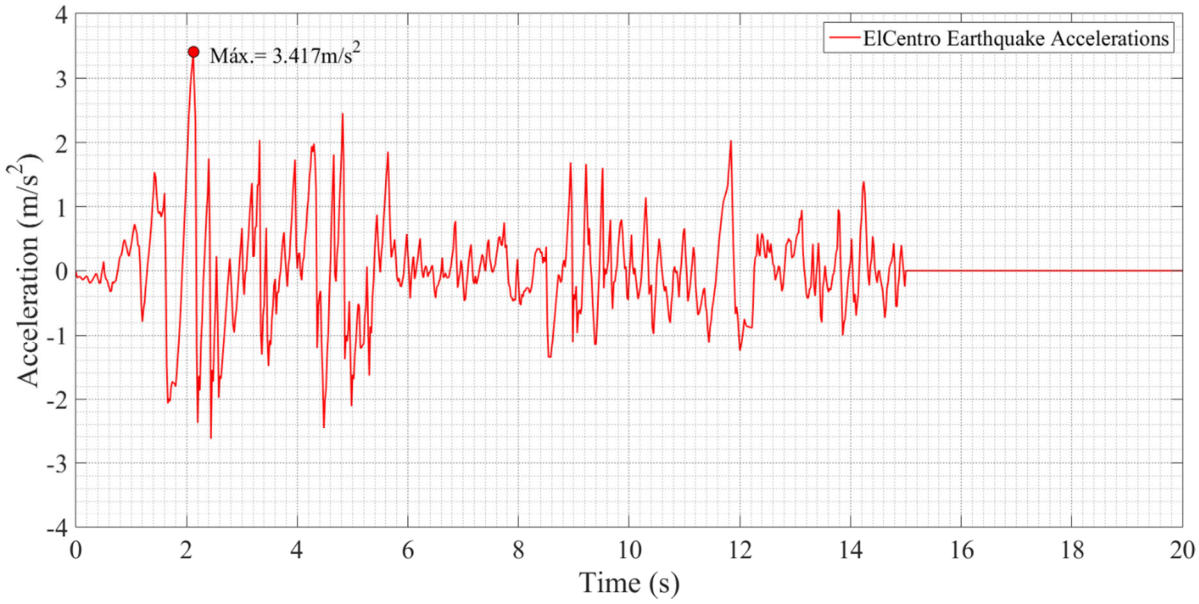

Fig. 3 - N-S component of El-Centro earthquake ground motion.

PLAIN HYSTERETIC BEHAVIOR (CASE 0)

A simple hysteretic behavior without degradation, suitable for well-detailed steel structures, e.g., special moment resisting frames (SMRFs), is represented by the following equations

$$P_f = k_f x = (a k_0 + k_{hyst}) x \tag{2}$$

$$k_{hyst} = (1-a) k_0 \left\{ 1 - \left| \frac{P_f}{P_{fy}} \right|^N \left[\eta \, sgn\left((1-a) P_f \dot{x} \right) + 1 - \eta \right] \right\} \tag{3}$$

where k_f is the nonlinear total lateral stiffness of the frame, k_0 is its initial lateral stiffness, a is the post-yield stiffness ratio, N a parameter that controls the transition smoothness from pre-yield to post-yield and η controls the shape of the discharge path. P_f and P_{fy} are the current frame shear and its yield value, respectively. Additionally, sgn is the signum function.

To determine the structural responses of the system represented in Figure 1 under the two signal accelerations considered, for each case of hysteretic behavior and each value of the mass ratio, it was used the numerical model previously mentioned above.

The graphs of Figures 4 to 7 shows the structural response of the system in study, considering the plain hysteretic behavior, subjected to the generic signal acceleration, for the values of the mass ratio $\mu = 0.05$, $\mu = 0.10$, $\mu = 0.15$ and $\mu = 0.20$, respectively, as well as graphs of Figures 10 to 13 but now when the system is subjected to the seismic acceleration.

The plain hysteretic behavior is described by the graphs of Figures 8 and 14 for the generic signal and seismic acceleration, respectively, where it shows the generalized force-displacement responses for the four different values of the mass ratio, comparing it with the corresponding uncontrolled case.

The response in terms of displacement of the TMD for different mass ratios, when the system represented in Figure 1 is subjected to the generic signal and seismic acceleration is described in Figures 9 and 15.

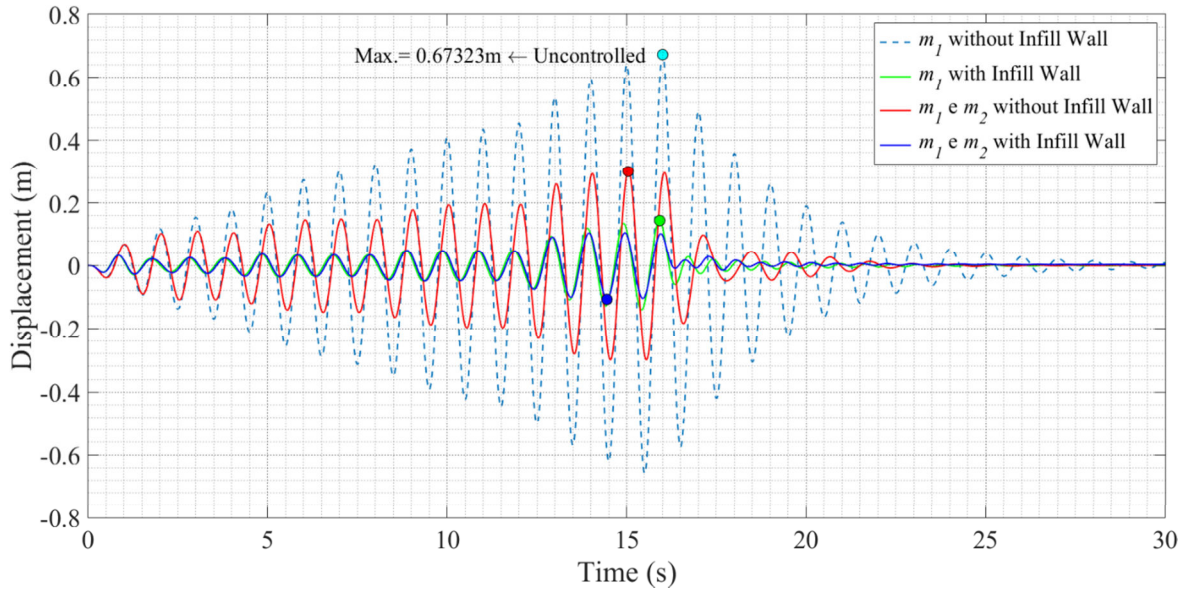

Fig. 4- Displacement responses of the structure controlled with a TMD with 5% of the structure mass, under the generic signal acceleration, considering Case 0 of hysteretic behavior.

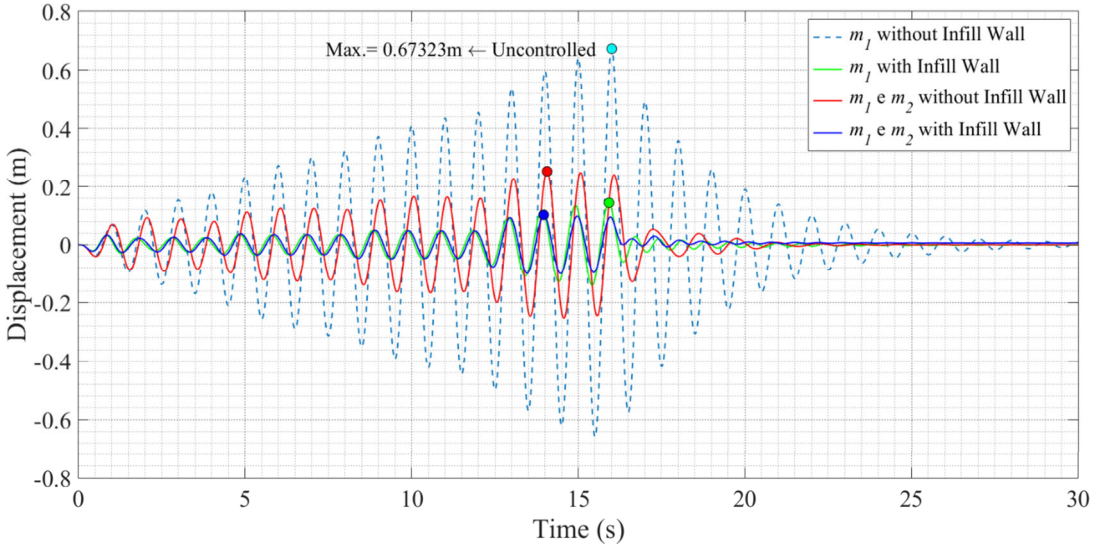

Fig. 5 - Displacement responses of the structure controlled with a TMD with 10% of the structure mass, under the generic signal acceleration, considering Case 0 of hysteretic behavior.

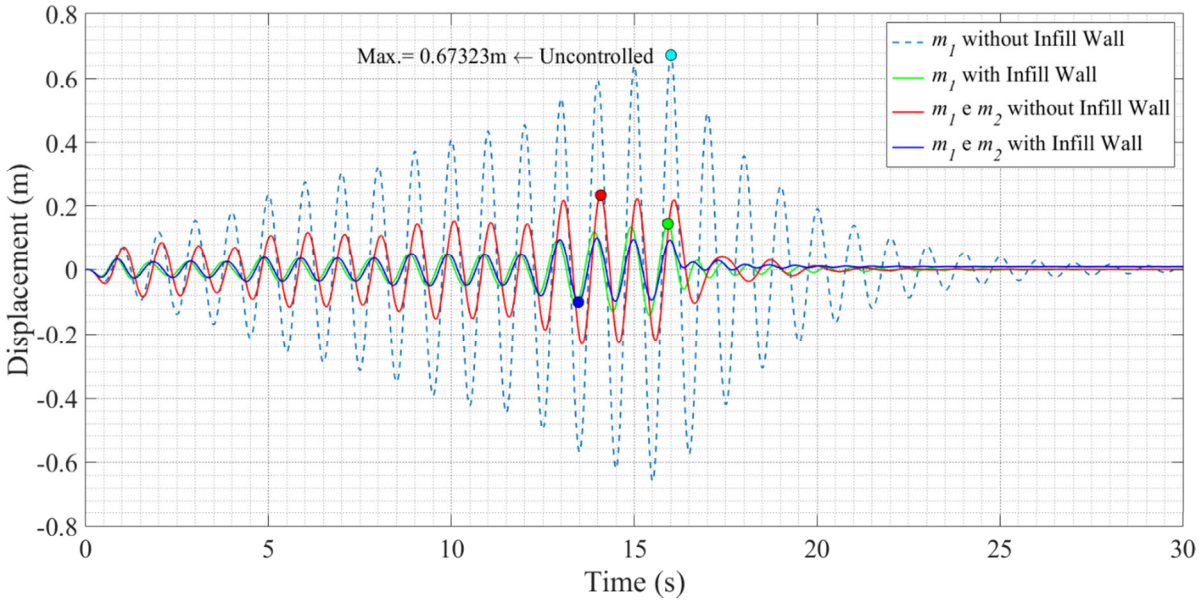

Fig. 6 - Displacement responses of the structure controlled with a TMD with 15% of the structure mass, under the generic signal acceleration, considering Case 0 of hysteretic behavior.

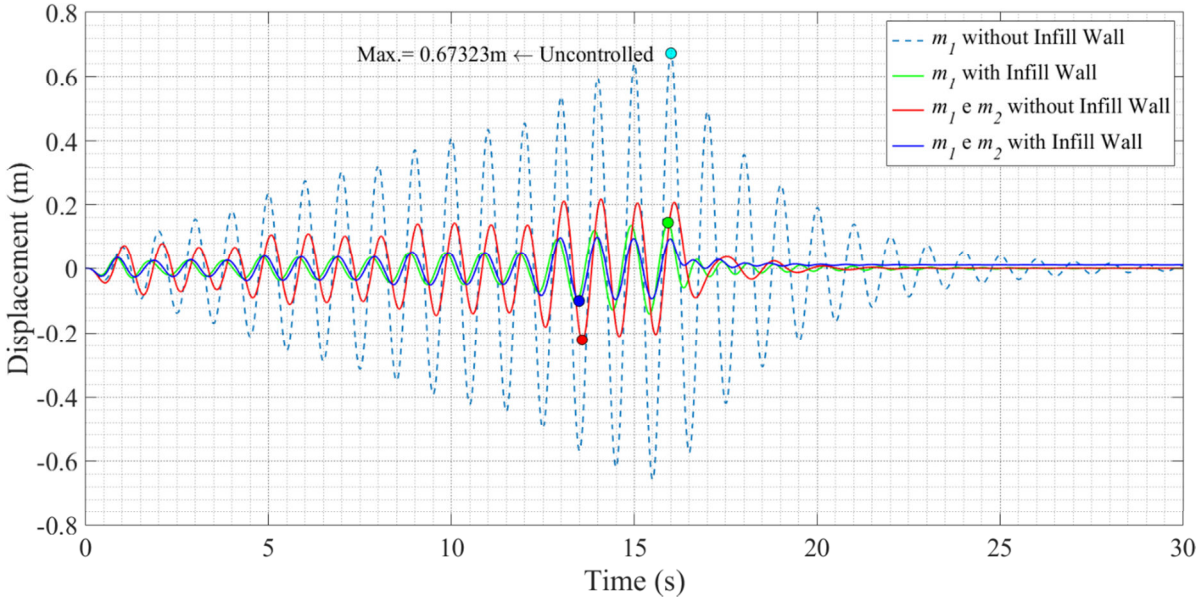

Fig. 7 - Displacement responses of the structure controlled with a TMD with 20% of the structure mass, under the generic signal acceleration, considering Case 0 of hysteretic behavior.

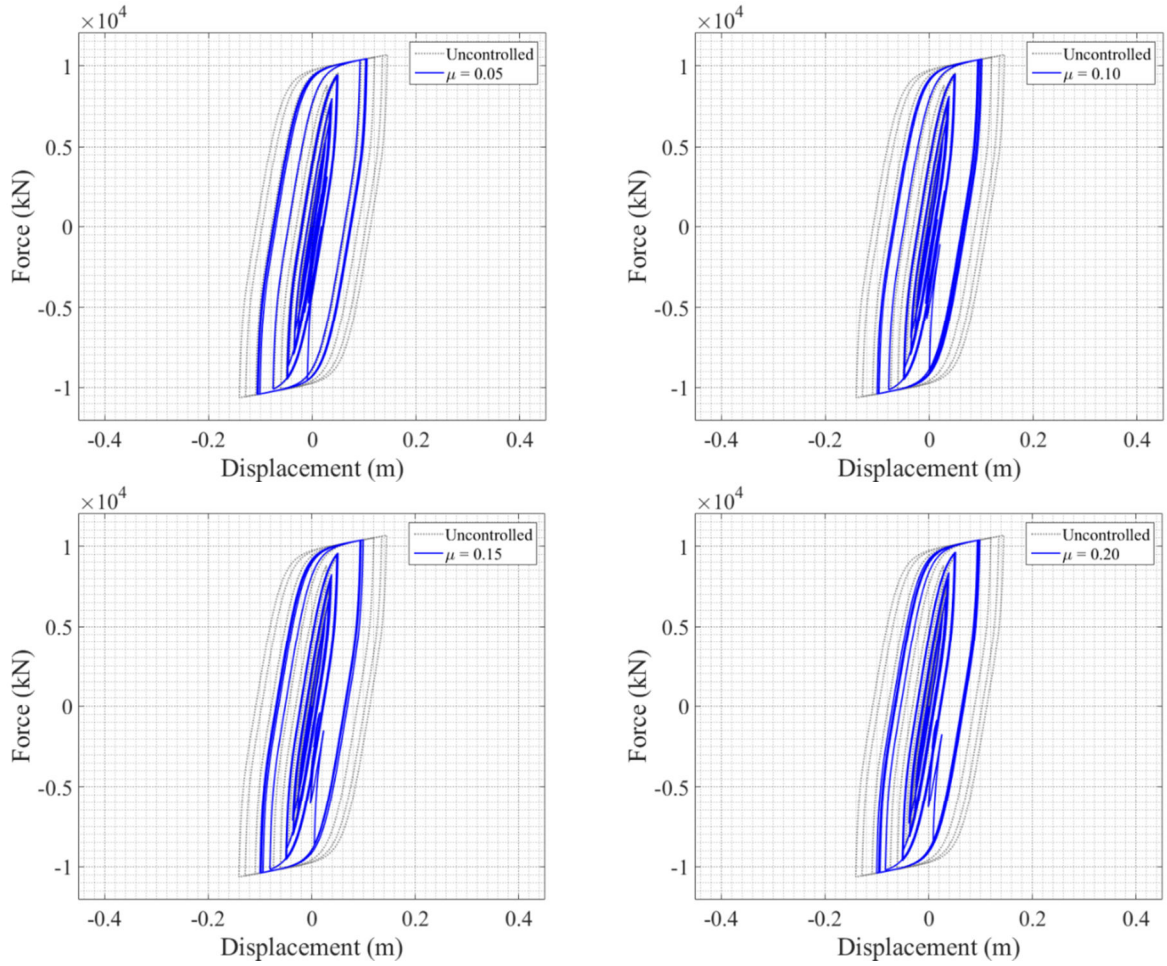

Fig. 8 - Hysteretic cycles of the infill wall structure under the generic signal acceleration, considering a plain hysteretic behavior (Case 0): (a) Mass Ratio of 5%; (b) Mass Ratio of 10%; (c) Mass Ratio of 15%; (d) Mass Ratio of 20%.

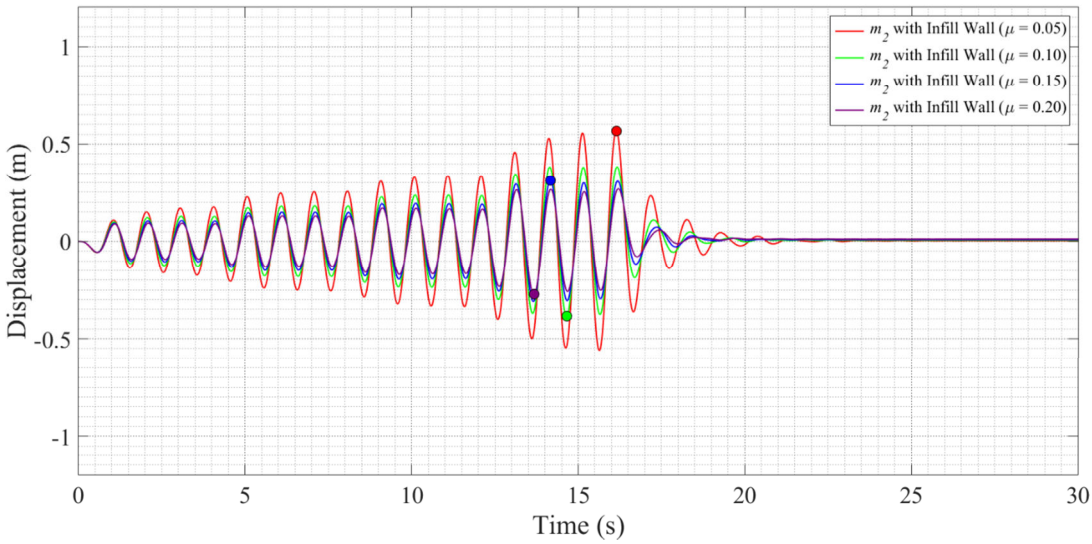

Fig. 9 - Displacement responses of the TMD for different values of the mass ratio, under the generic signal acceleration, considering Case 0 of hysteretic behavior.

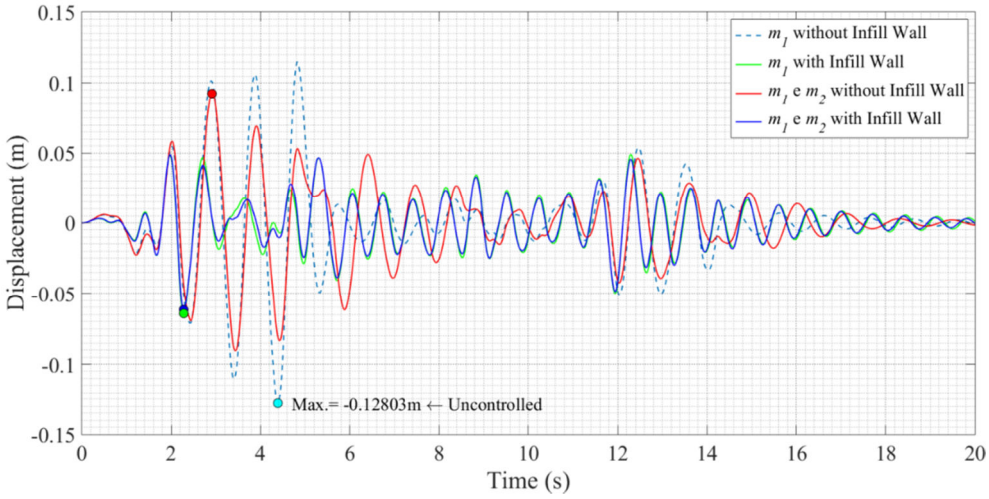

Fig. 10 - Displacement responses of the structure with a TMD with 5% of the structure mass under the seismic acceleration, considering Case 0 of hysteretic behavior.

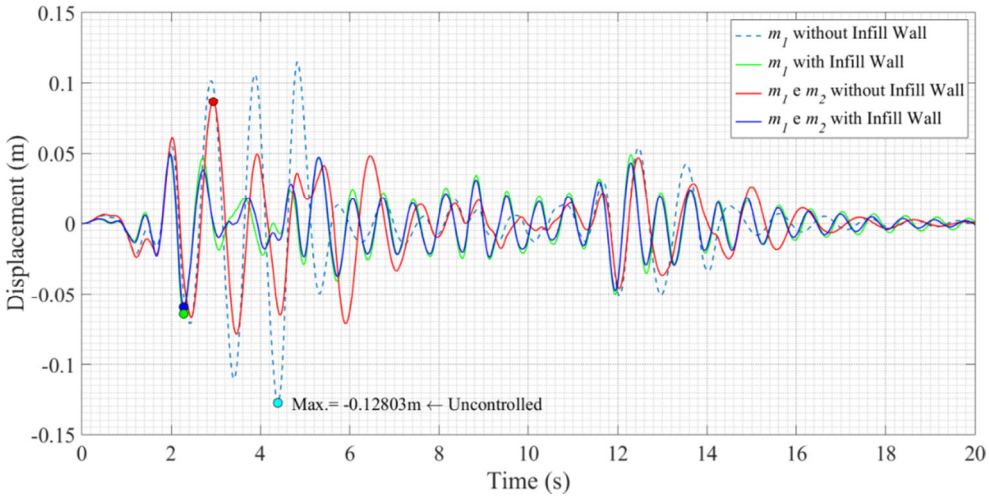

Fig. 11 - Displacement responses of the structure with a TMD with 10% of the structure mass under the seismic acceleration, considering Case 0 of hysteretic behavior.

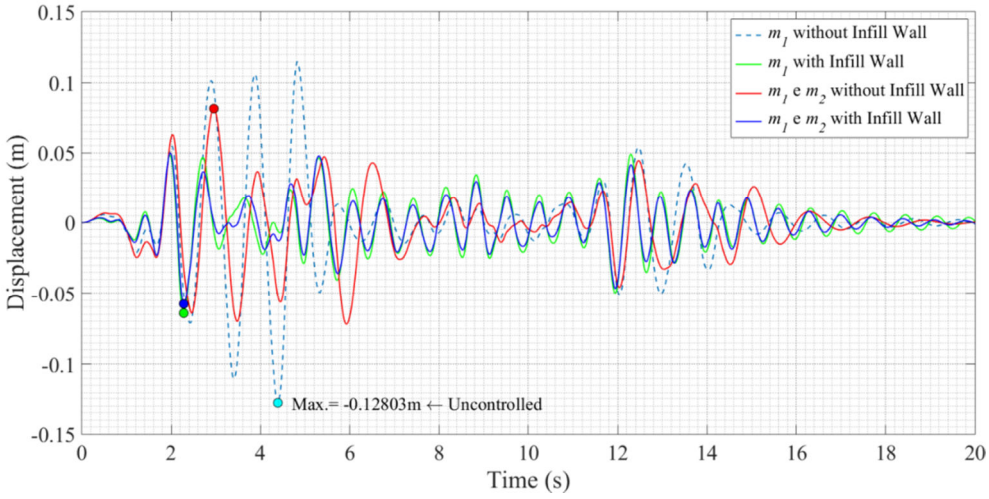

Fig. 12 - Displacement responses of the structure with a TMD with 15% of the structure mass under the seismic

acceleration, considering Case 0 of hysteretic behavior.

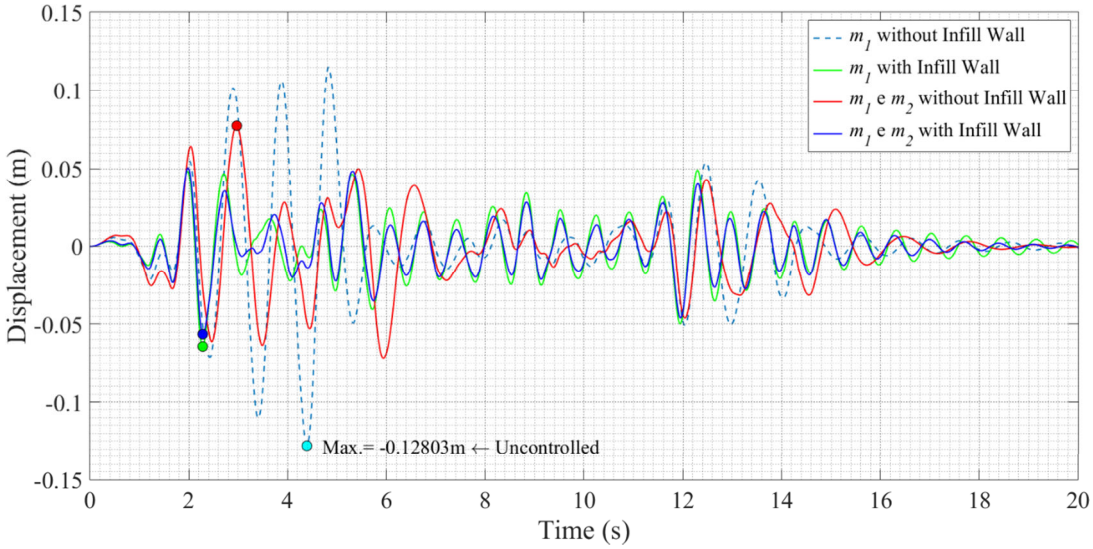

Fig. 13 - Displacement responses of the structure with a TMD with 20% of the structure mass under the seismic acceleration, considering Case 0 of hysteretic behavior.

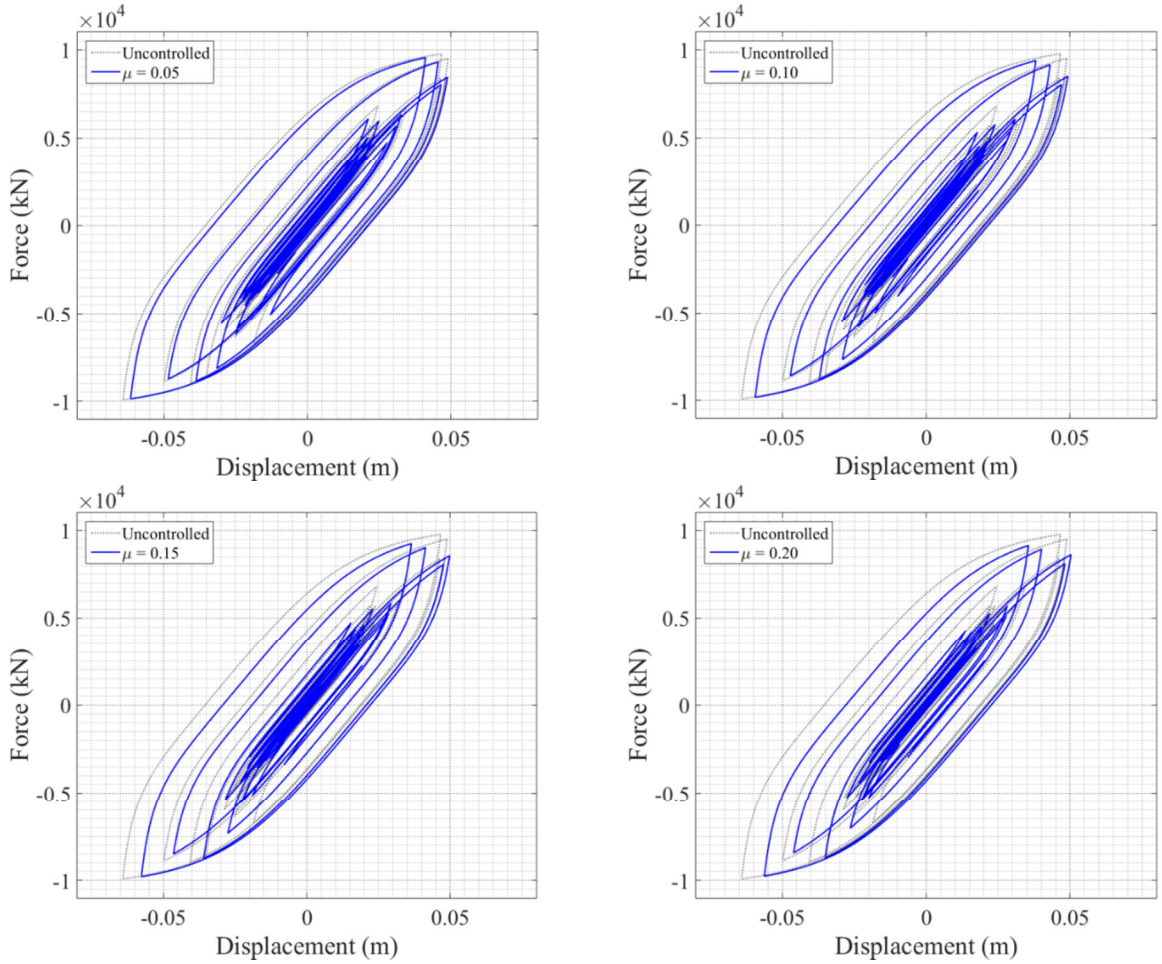

Fig. 14 - Hysteretic cycles of the infill wall structure under the seismic acceleration, considering a plain hysteretic behavior (Case 0): (a) Mass ratio of 5%; (b) Mass ratio of 10%; (c) Mass ratio of 15%; (d) Mass ratio of 20%.

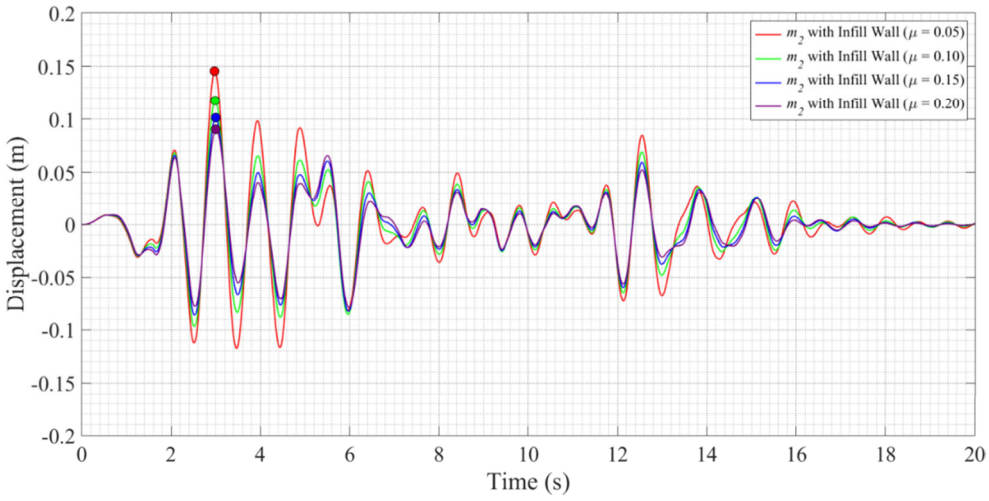

Fig. 15 - Displacement responses of the TMD for different values of the mass ratio, under the seismic acceleration, considering Case 0 of hysteretic behavior.

STIFFNESS DEGRADATION (CASE I)

The stiffness degradation arises from geometric effects. Elastic stiffness reduces with increased ductility. The stiffness degradation is implemented in the Macro-Simulink model through the so-called pivot rule (Park *et al*., 1987). Most reinforced concrete undergoes stiffness degradation that should be accounted in a nonlinear dynamic analysis. To address this case, k_{hyst} should be modified as follows

$$k_{hyst} = (R_k - a)k_0\left\{1 - \left|\frac{P_f}{P_{fy}}\right|^N \left[\eta\,\mathrm{sgn}\left((1-a)P_f\dot{x}\right) + 1 - \eta\right]\right\} \tag{4}$$

where

$$P_f = k_f x = (ak_0 + k_{hyst})x \tag{5}$$

$$R_k = \frac{P_f + \alpha P_{fy}}{k_0 x + \alpha P_{fy}} \tag{6}$$

The parameter α can regulate the stiffness degradation. The higher the α, the lower the stiffness degradation. It should be pointed out that R_k in Equation 4 is a positive parameter and the unit is its maximum possible value. Nevertheless, R_k is also a decreasing function of time, since the stiffness of the structure would not increase after deterioration, regardless of the current displacement.

The stiffness degradation can be simulated using the Equations 4, 5 and 6, with the respective values presented in Table 1. Applying these considerations in the numerical model in study, the structural responses can be obtained for the two signal accelerations considered in the present study.

The structural responses obtained for the generic signal and seismic acceleration, for the different values of the mass ratio considered are presented in Figures 16 to 19 and Figures 22 to 25, respectively. The responses in terms of displacements concerning only the TMD are shown in Figures 21 and 26, respectively for the generic signal and seismic acceleration. The graphs showing the hysteretic behavior for different values of the mass ratio are presented in Figures 20 and 27, respectively for the generic signal and seismic acceleration.

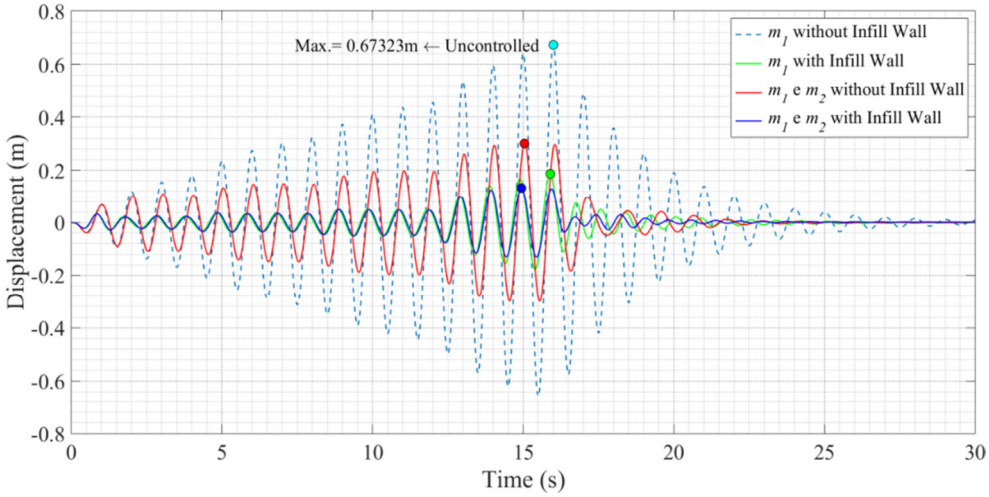

Fig. 16 - Displacement responses of the structure controlled with a TMD with 5% of the structure mass, under the generic signal acceleration, considering Case I of hysteretic behavior.

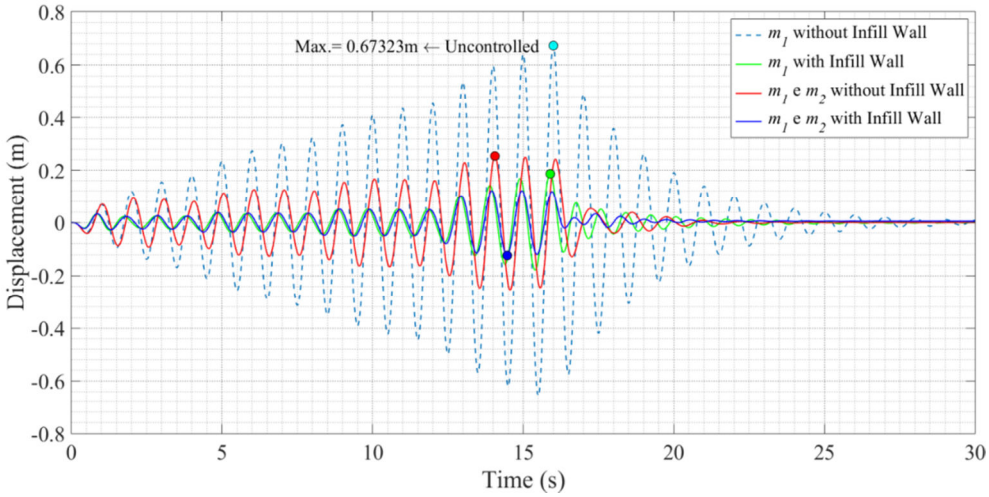

Fig. 17 - Displacement responses of the structure controlled with a TMD with 10% of the structure mass, under the generic signal acceleration, considering Case I of hysteretic behavior.

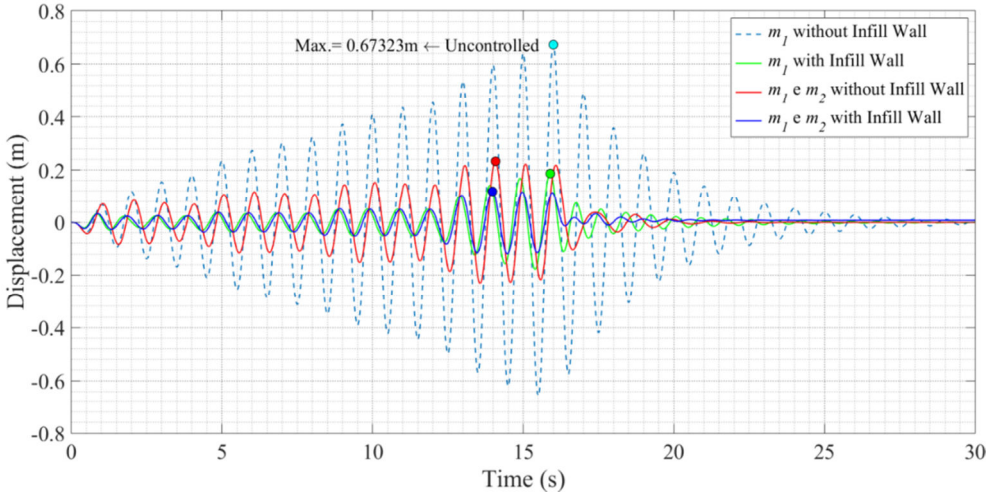

Fig. 18 - Displacement responses of the structure controlled with a TMD with 15% of the structure mass, under the generic signal acceleration, considering Case I of hysteretic behavior.

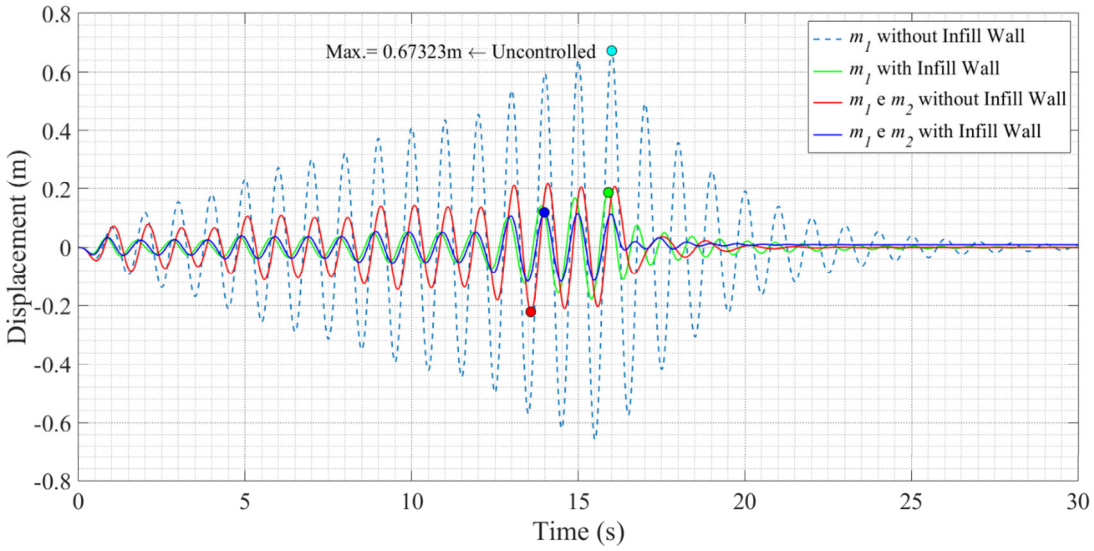

Fig. 19 - Displacement responses of the structure controlled with a TMD with 20% of the structure mass, under the generic signal acceleration, considering Case I of hysteretic behavior.

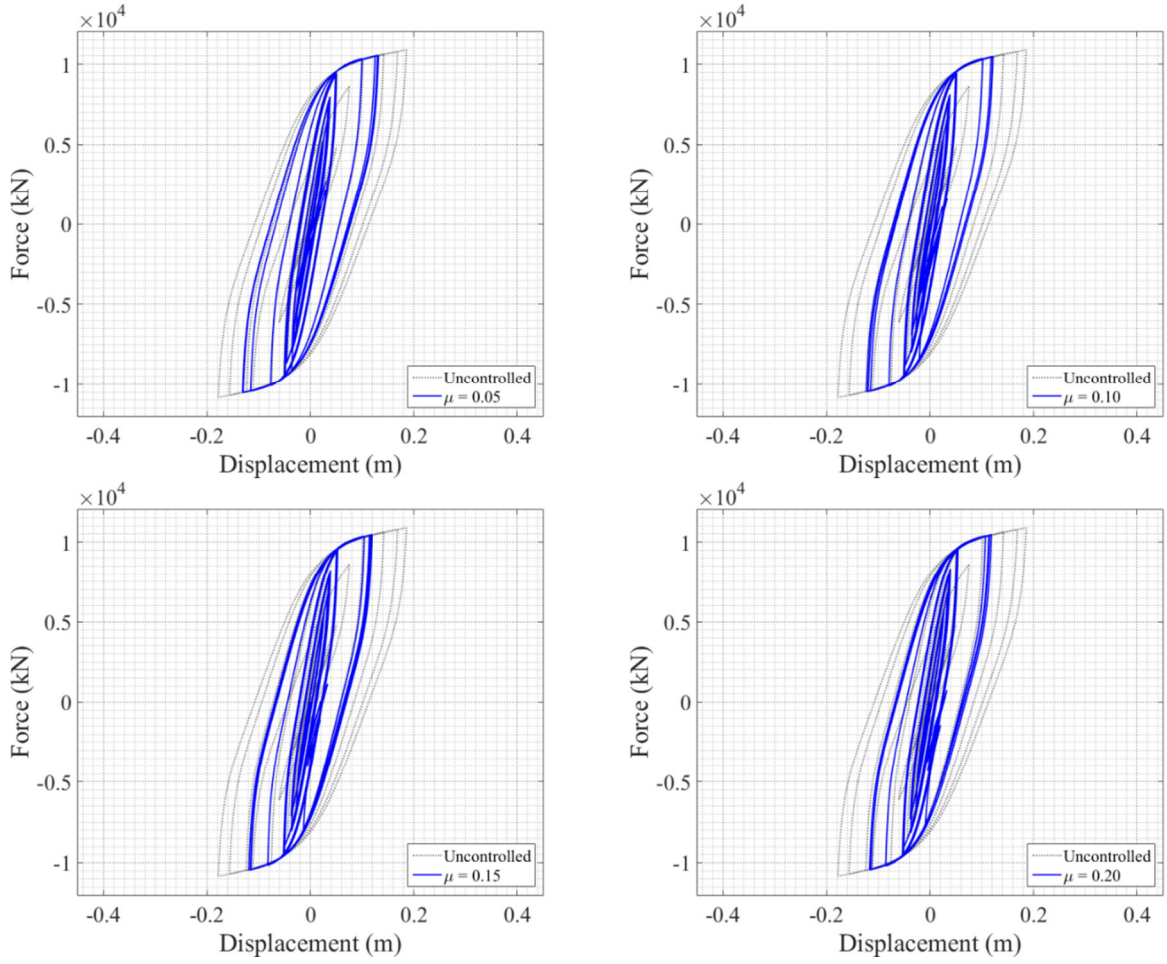

Fig. 20 - Hysteretic cycles of the infill wall structure under the generic signal acceleration, considering the stiffness degradation (Case I): (a) Mass Ratio of 5%; (b) Mass Ratio of 10%; (c) Mass Ratio of 15%; (d) Mass Ratio of 20%.

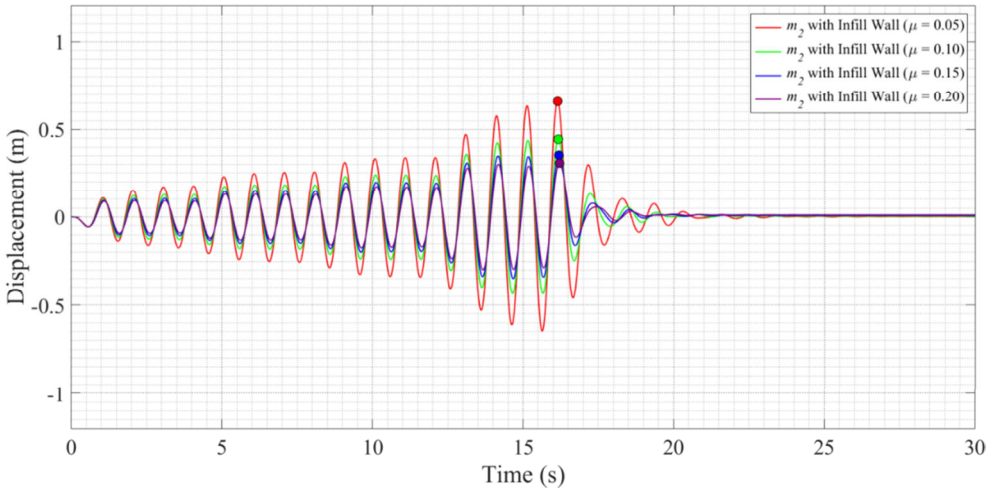

Fig. 21 - Displacement responses of the TMD for different values of the mass ratio, under the generic signal acceleration, considering Case I of hysteretic behavior.

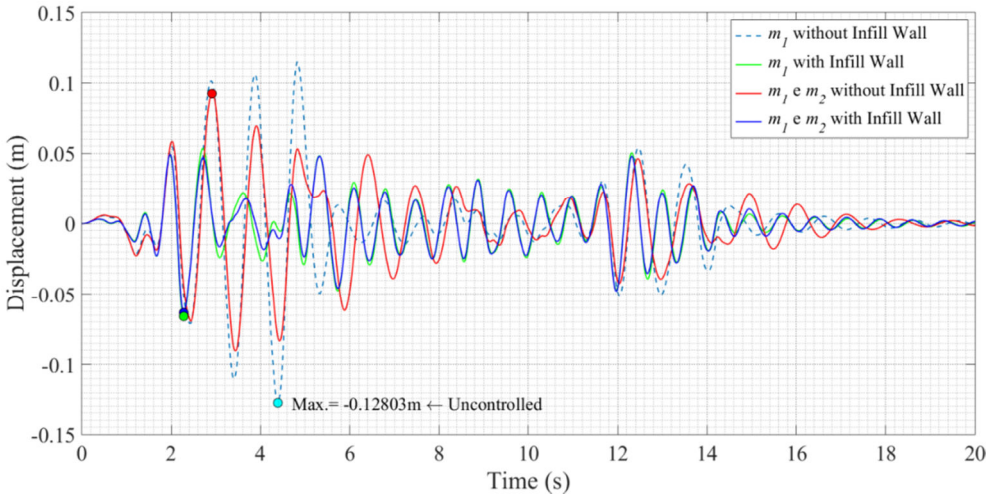

Fig. 22 - Displacement responses of the structure with a TMD with 5% of the structure mass under the seismic acceleration, considering Case I of hysteretic behavior.

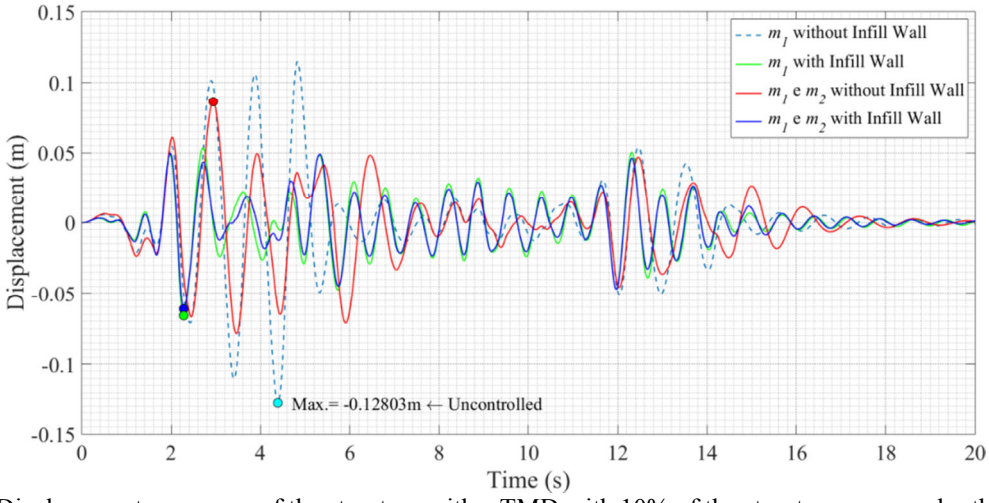

Fig. 23 - Displacement responses of the structure with a TMD with 10% of the structure mass under the seismic acceleration, considering Case I of hysteretic behavior.

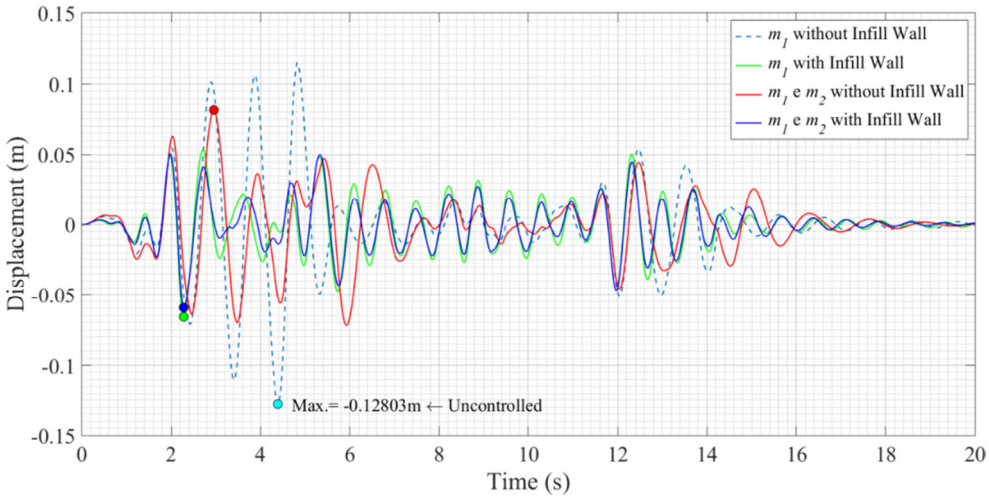

Fig. 24 - Displacement responses of the structure with a TMD with 15% of the structure mass under the seismic acceleration, considering Case I of hysteretic behavior.

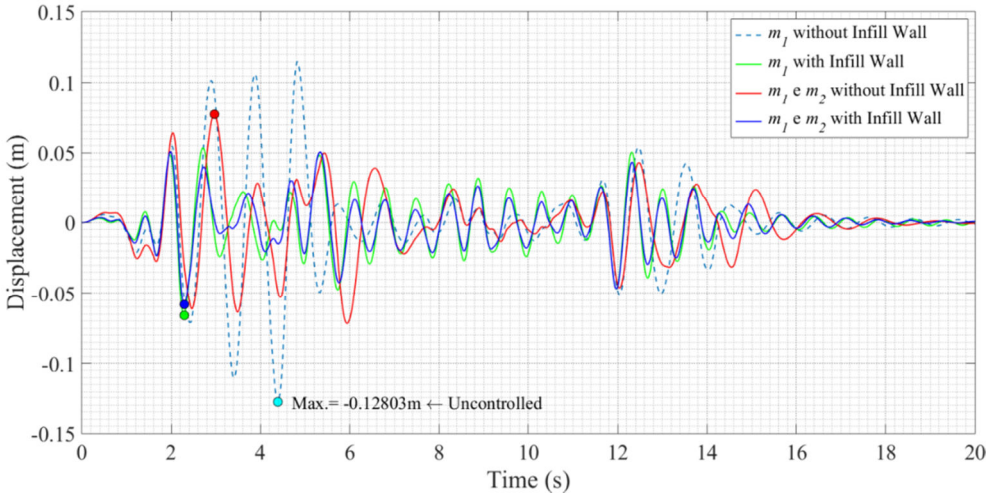

Fig. 25 - Displacement responses of the structure with a TMD with 20% of the structure mass under the seismic acceleration, considering Case I of hysteretic behavior.

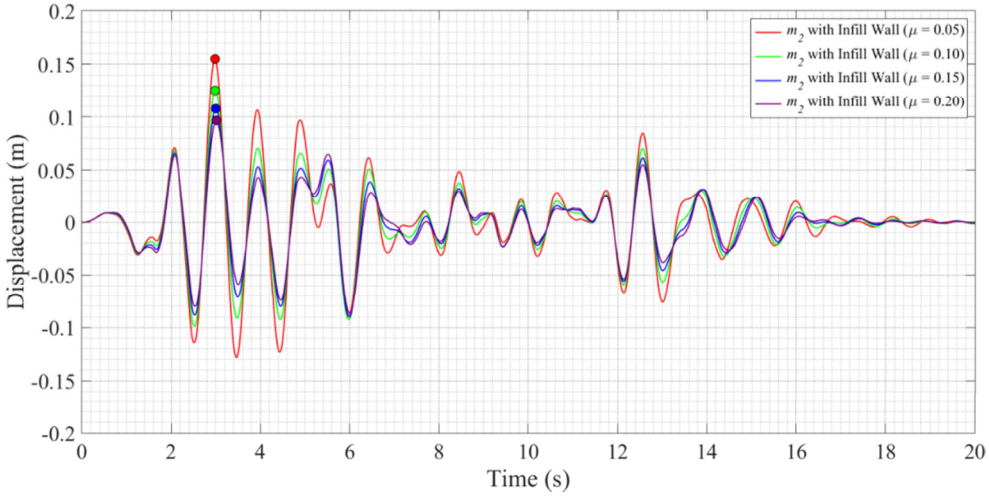

Fig. 26 - Displacement responses of the TMD for different values of the mass ratio, under the seismic acceleration, considering Case I of hysteretic behavior.

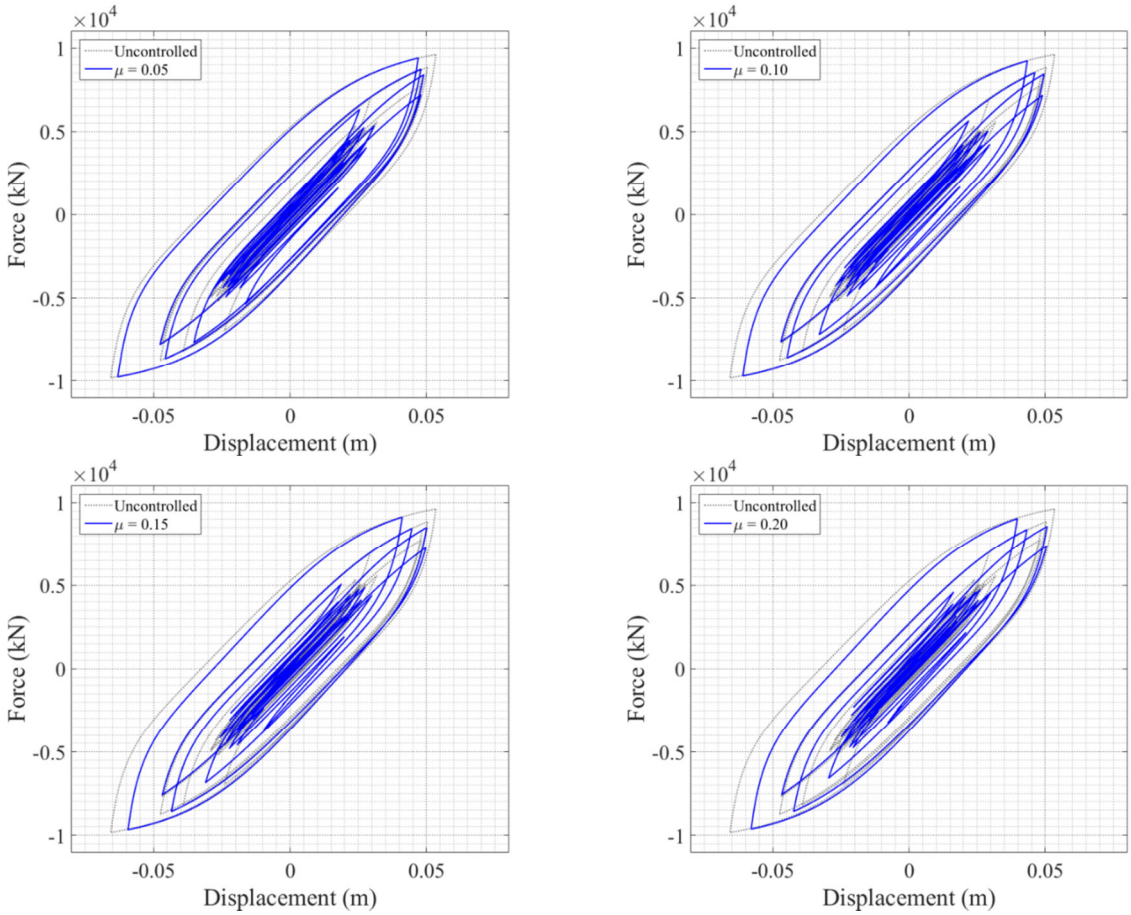

Fig. 27 - Hysteretic cycles of the infill wall structure under the seismic acceleration, considering the stiffness degradation (Case I): (a) Mass Ratio of 5%; (b) Mass Ratio of 10%; (c) Mass Ratio of 15%; (d) Mass Ratio of 20%.

STIFFNESS AND STRENGTH DEGRADATION (CASE II)

To counteract the P-Δ effects, as well as the strength deterioration during repeated load inversions, a degradation of resistance based on energy/ductility is implemented in the Macro-Simulink model. This is achieved by the following modification on the yield strength.

$$P_{fy} = P_{fy0}\left[1-\left(\frac{x_{max}}{x_{ult}}\right)^{\frac{1}{\beta_1}}\right]\left[1-\frac{\beta_2 H}{(1-\beta_2)H_{ult}}\right] \quad (7)$$

The degraded and initial yielding strength of the frame are indicated by P_{fy} and P_{fy0}, respectively. The parameters $u_{\max}$ and u_{ult} are the maximum displacement in the current load inversion and the ultimate displacement capacity of the frame, respectively. The dissipated energy accumulated at the current displacement is represented by H and H_{ult} is the ultimate dissipated energy under monotonic (non-cyclic) load. Furthermore, β_1 and β_2 are degradation parameters based on ductility and energy dissipation demands, respectively.

Strength degradation should be considered for ordinary or intermediate moment resisting frames under great ductility demands. Most reinforced concrete frames and shear walls would also experience strength deterioration.

The stiffness and strength degradation can be simulated by using the respective values of Table 1 in the Equation 7. By doing this, the structural responses of the system illustrated in Figure1, subjected to the two accelerations, can be computed.

The responses in terms of displacements of the system under the generic signal acceleration are presented in Figures 28 to 31 for the different values considered of the mass ratio. In like manner, for the responses to the seismic acceleration are shown in Figures 34 to 37, for the same values of the mass ratio considered.

The displacements of only the TMD, when the structure where it is applied is requested by the generic signal acceleration can be seen in Figure 32 for the different contemplated values of the mass ratio. The responses of only the TMD for the different values of mass ratio, when the system is subjected by the seismic acceleration can be observed in Figure 38.

The hysteretic loops in which the stiffness and strength degradation are considered are shown in Figures 33 and 39, respectively for the generic signal and seismic acceleration, and for the different contemplated values of mass ratio.

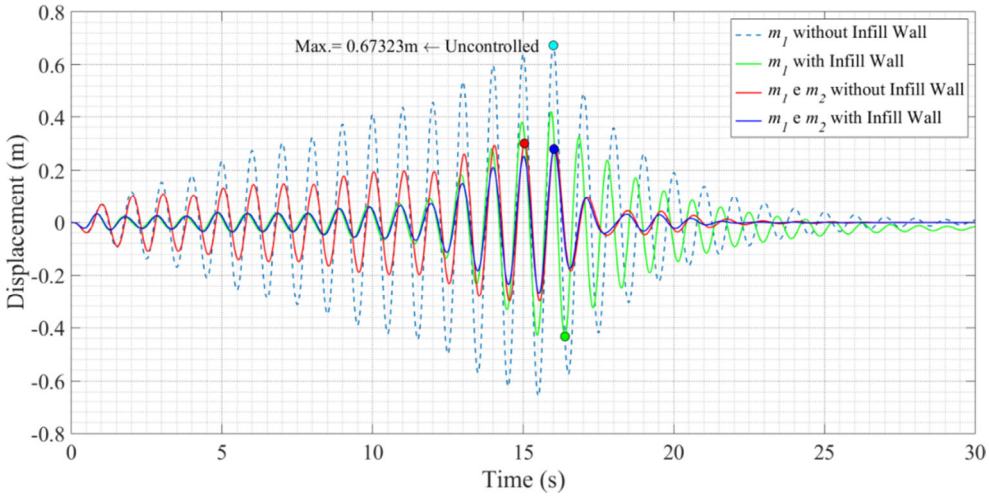

Fig. 28 - Displacement responses of the structure controlled with a TMD with 5% of the structure mass, under the generic signal acceleration, considering Case II of hysteretic behavior.

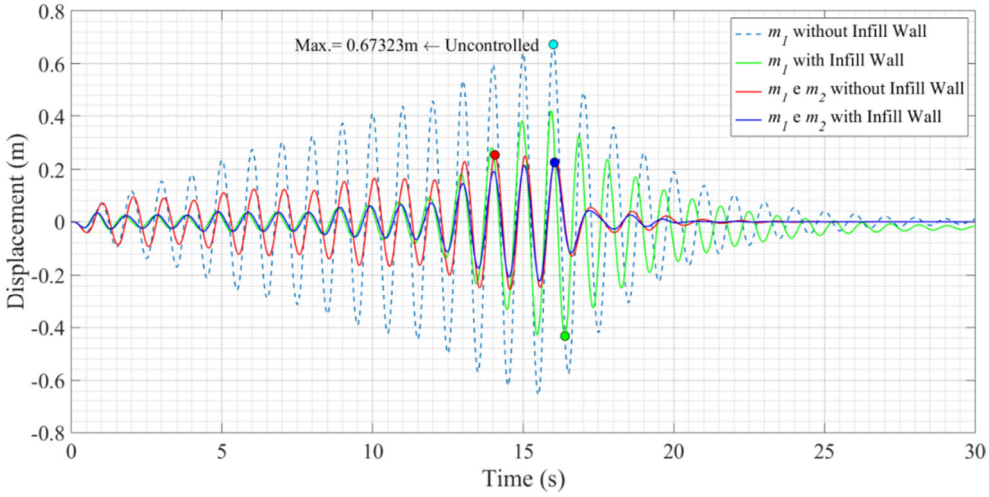

Fig. 29 - Displacement responses of the structure controlled with a TMD with 10% of the structure mass, under the generic signal acceleration, considering Case II of hysteretic behavior.

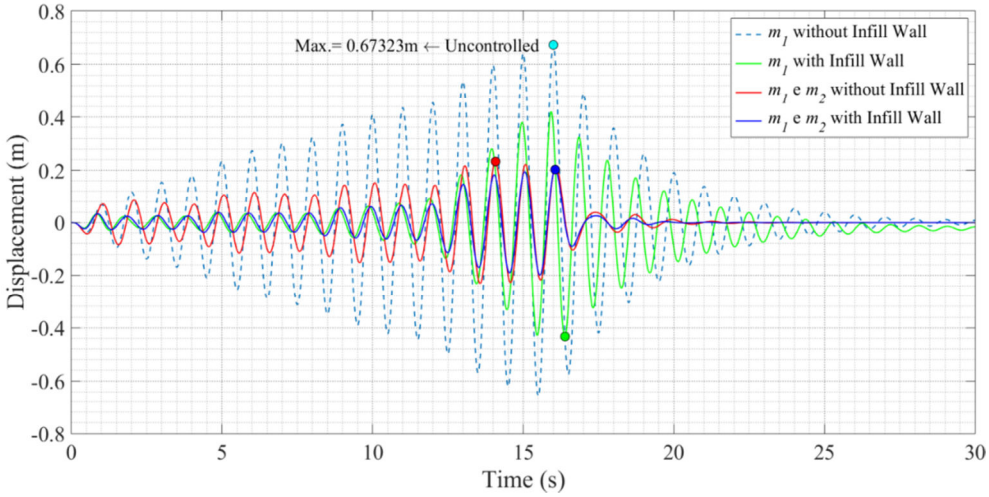

Fig. 30- Displacement responses of the structure controlled with a TMD with 15% of the structure mass, under the generic signal acceleration, considering Case II of hysteretic behavior.

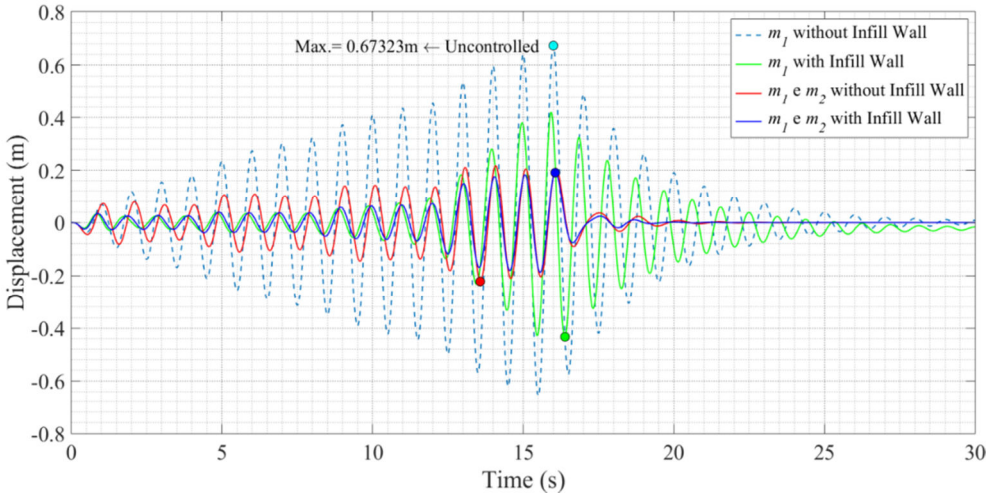

Fig. 31 - Displacement responses of the structure controlled with a TMD with 20% of the structure mass, under the generic signal acceleration, considering Case II of hysteretic behavior.

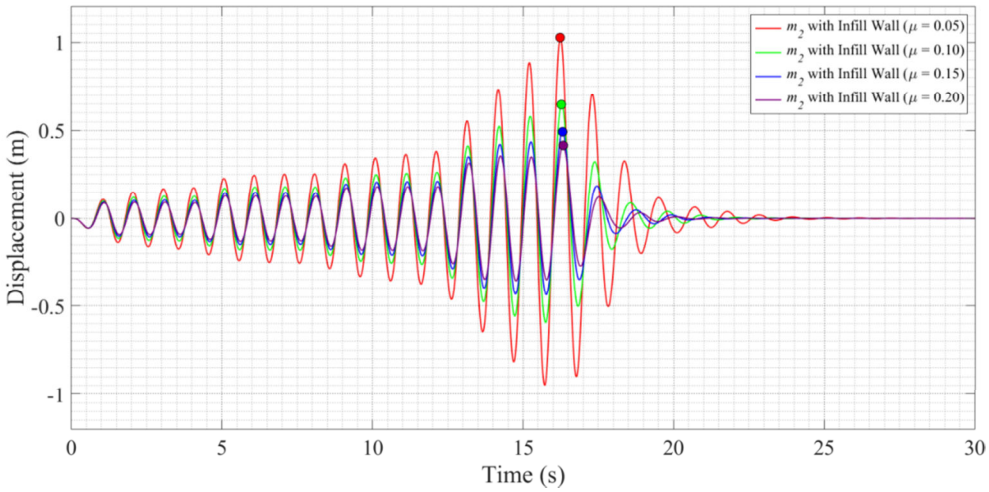

Fig. 32 - Displacement responses of the TMD for different values of the mass ratio, under the generic signal acceleration, considering Case II of hysteretic behavior.

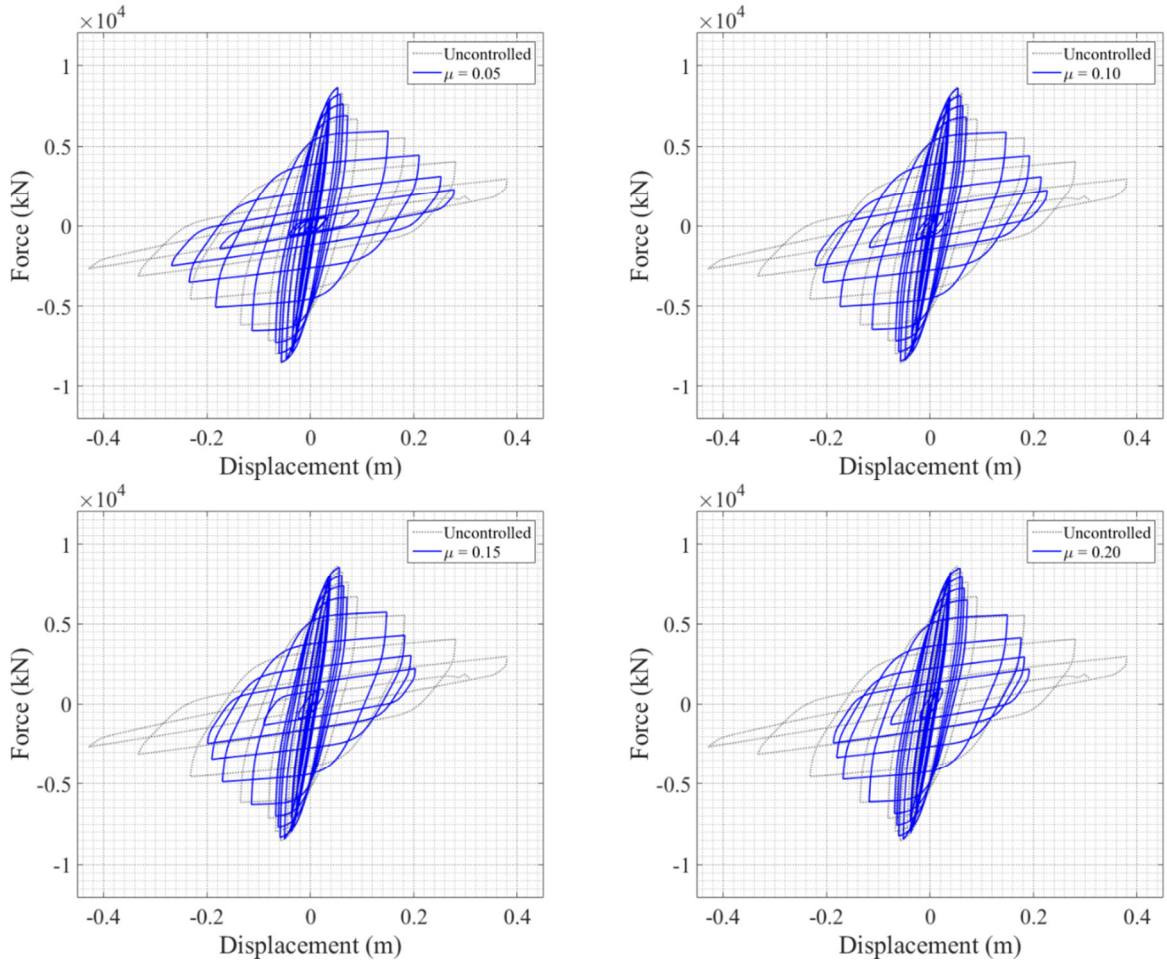

Fig. 33 - Hysteretic cycles of the infill wall structure under the generic signal acceleration, considering the stiffness and strength degradation (Case II): (a) Mass Ratio of 5%; (b) Mass Ratio of 10%; (c) Mass Ratio of 15%; (d) Mass Ratio of 20%.

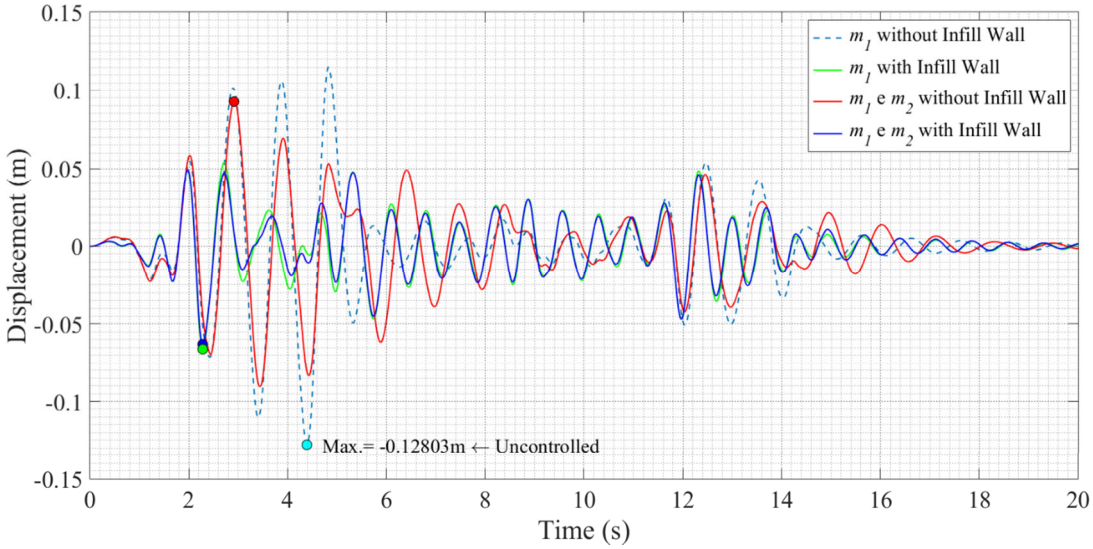

Fig. 34 - Displacement responses of the structure with a TMD with 5% of the structure mass under the seismic acceleration, considering Case II of hysteretic behavior.

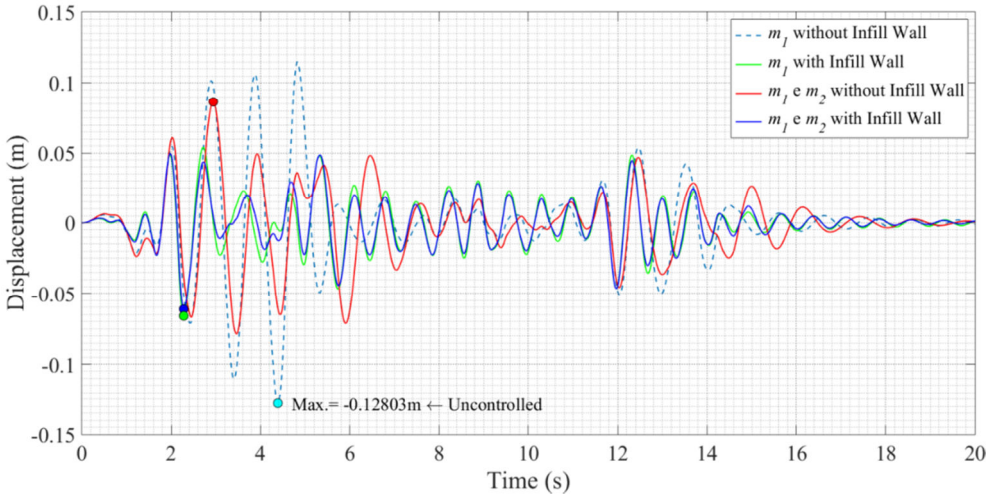

Fig. 35 - Displacement responses of the structure with a TMD with 10% of the structure mass under the seismic acceleration, considering Case II of hysteretic behavior.

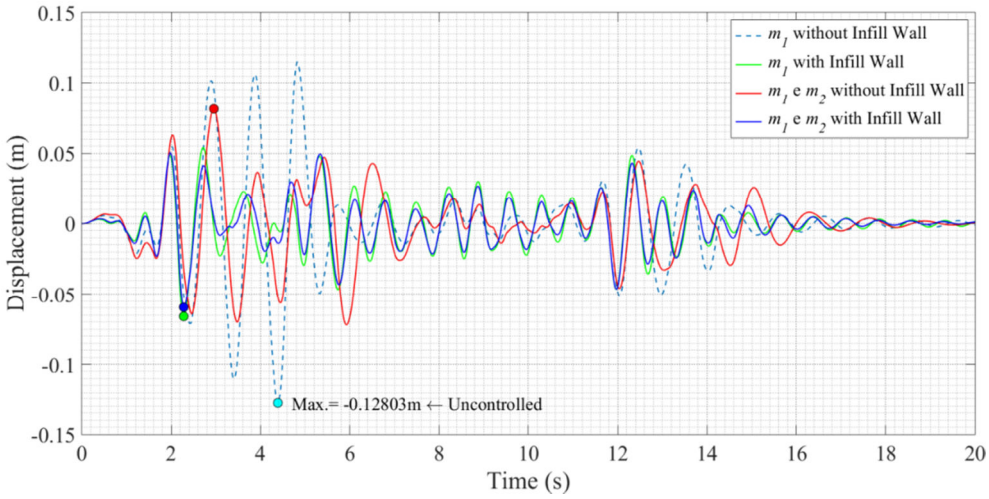

Fig. 36 - Displacement responses of the structure with a TMD with 15% of the structure mass under the seismic acceleration, considering Case II of hysteretic behavior.

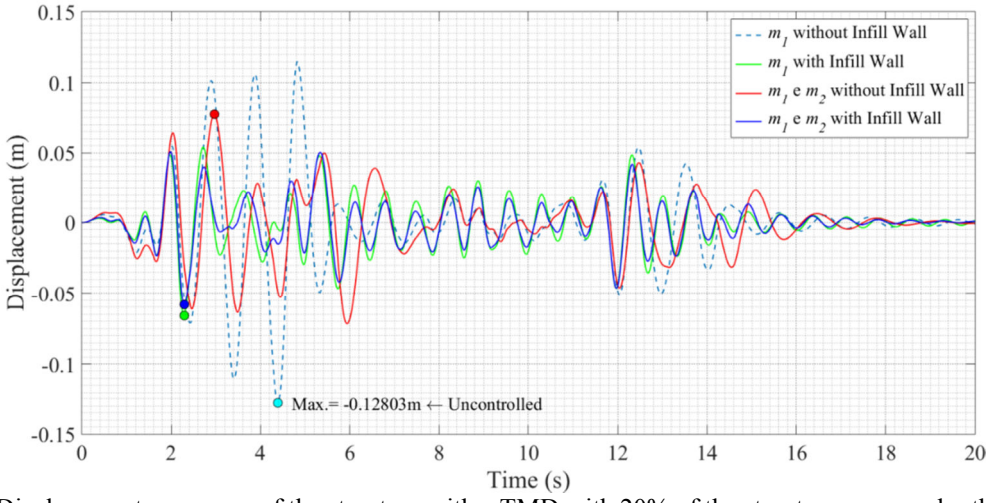

Fig. 37 - Displacement responses of the structure with a TMD with 20% of the structure mass under the seismic acceleration, considering Case II of hysteretic behavior.

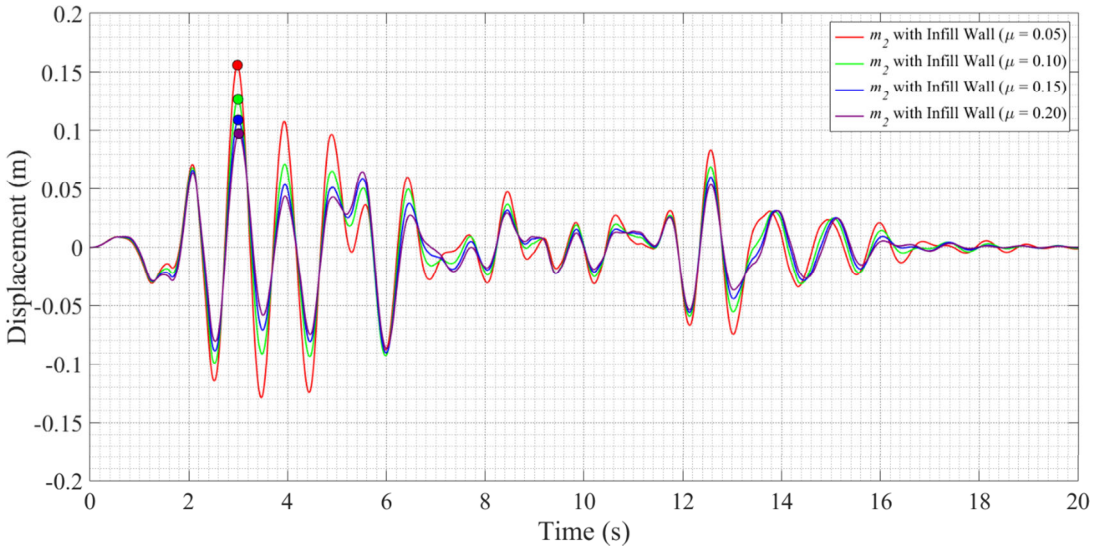

Fig. 38 - Displacement responses of the TMD for different values of the mass ratio, under the seismic acceleration, considering Case II of hysteretic behavior.

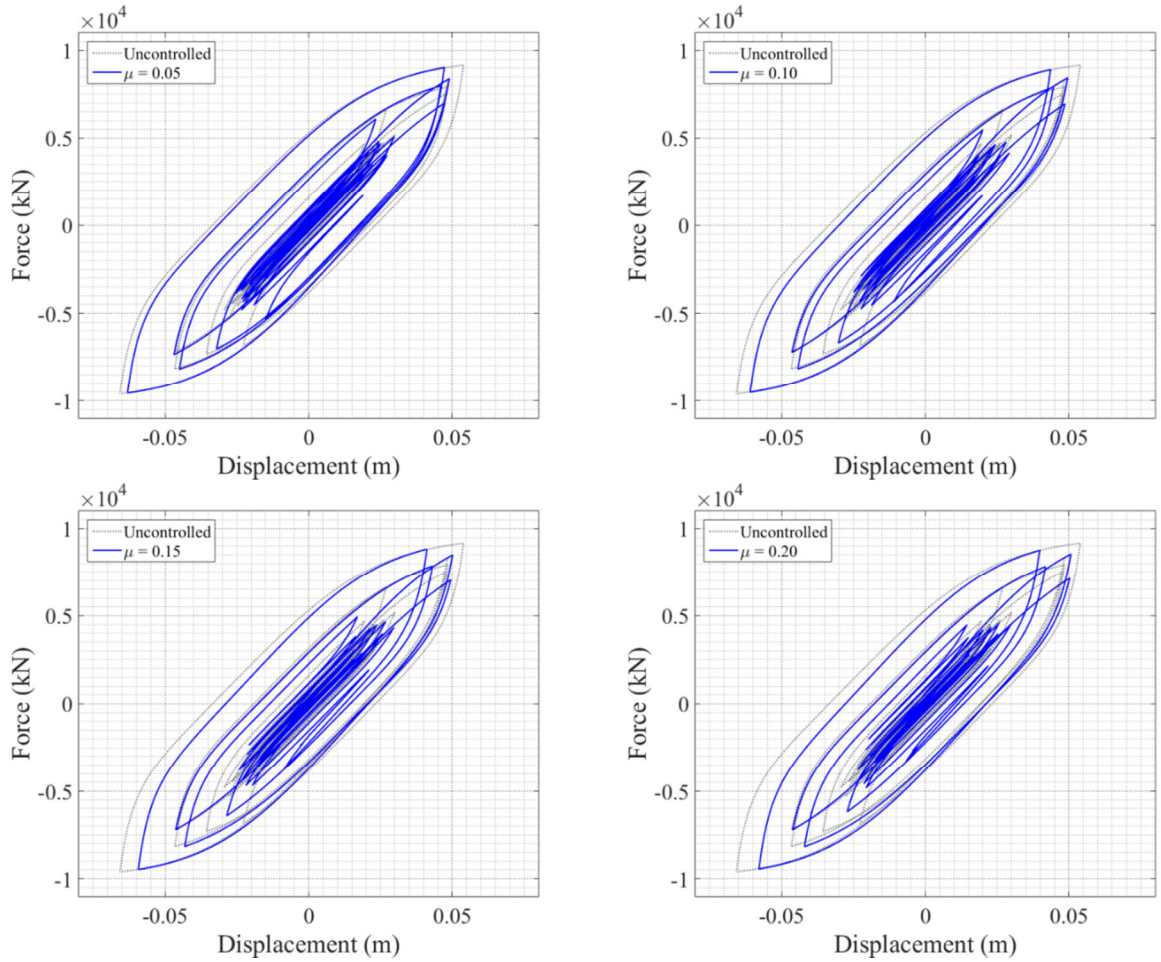

Fig. 39 - Hysteretic cycles of the infill wall structure under the seismic acceleration, considering the stiffness and strength degradation (Case II): (a) Mass Ratio of 5%; (b) Mass Ratio of 10%; (c) Mass Ratio of 15%; (d) Mass Ratio of 20%.

RESULTS AND COMMENTS

The results of the peak responses that contemplate the displacements, velocities, accelerations and drift displacements of the system represented in Figure 1, for the three different cases of hysteretic behavior and different values of the mass ratio between the TMD and the structure, are presented in the Tables 2 and 3, for the generic signal and seismic acceleration, respectively.

Observing the Table 2, it can be always verified, when comparing it with other mass ratios, that the mass ratio of 20% offers the best results in reducing any type of the peak responses, following by the mass ratio of 15% which in some cases the variation is very small when comparing it with the case without infill wall. It can also be concluded that as it moves on to a case of hysteretic behavior more realistic the percentages of reduction become smaller.

Table 2 - Peak responses of the structure under the generic signal acceleration.

Peak responses						
Case of Hysteretic behavior		**Mass ratio**	x (m)	$\dot{x}$ (m/s)	$\ddot{x}$ (m/s^2)	drift (m)
Without infill wall		**0.05**	0.301 1.127	1.882 6.719	11.795 41.796	0.301 1.064
		0.10	0.254 0.681	1.584 3.968	9.891 24.758	0.254 0.637
		0.15	0.233 0.512	1.443 2.947	9.007 18.267	0.233 0.484
		0.20	0.221 0.431	1.363 2.398	8.457 14.821	0.221 0.408
With infill wall	**Case 0**	**0.05**	0.106 (-183%) 0.567 (-99%)	0.643 (-193%) 3.501 (-92%)	4.680 (-152%) 21.910 (-91%)	0.106 (-183%) 0.528 (-102%)
		0.10	0.101 (-150%) 0.383 (-78%)	0.613 (-158%) 2.383 (-67%)	4.453 (-122%) 14.943 (-66%)	0.101 (-150%) 0.355 (-80%)
		0.15	0.100 (-133%) 0.311 (-65%)	0.604 (-139%) 1.918 (-54%)	4.406 (-104%) 11.997 (-52%)	0.100 (-133%) 0.285 (-70%)
		0.20	0.100 (-120%) 0.272 (-59%)	0.604 (-126%) 1.659 (-45%)	4.393 (-93%) 10.326 (-44%)	0.100 (-120%) 0.247 (-65%)
	Case I	**0.05**	0.132 (-128%) 0.661 (-70%)	0.819 (-130%) 4.066 (-65%)	5.520 (-114%) 25.237 (-66%)	0.132 (-128%) 0.623 (-71%)
		0.10	0.123 (-106%) 0.444 (-54%)	0.762 (-108%) 2.730 (-45%)	5.158 (-92%) 17.109 (-45%)	0.123 (-106%) 0.414 (-54%)
		0.15	0.120 (-94%) 0.353 (-45%)	0.743 (-94%) 2.171 (-36%)	5.031 (-79%) 13.576 (-35%)	0.120 (-94%) 0.331 (-46%)
		0.20	0.119 (-86%) 0.306 (-41%)	0.735 (-85%) 1.862 (-29%)	4.987 (-70%) 11.616 (-28%)	0.119 (-86%) 0.286 (-43%)
	Case II	**0.05**	0.278 (-8%) 1.027 (-10%)	1.699 (-11%) 5.977 (-12%)	10.653 (-11%) 35.704 (-17%)	0.278 (-8%) 0.948 (-12%)
		0.10	0.227 (-12%) 0.648 (-5%)	1.395 (-14%) 3.697 (-7%)	8.739 (-13%) 22.541 (-10%)	0.227 (-12%) 0.594 (-7%)
		0.15	0.203 (-14%) 0.493 (-4%)	1.252 (-15%) 2.725 (-8%)	7.908 (-14%) 16.796 (-9%)	0.203 (-14%) 0.451 (-8%)
		0.20	0.192 (-15%) 0.415 (-4%)	1.178 (-16%) 2.209 (-9%)	7.460 (-13%) 13.630 (-9%)	0.192 (-15%) 0.378 (-8%)

c. The first and second lines represent the peak responses for the first and second floors, respectively, the main structure and the TMD.

d. The percentage on the left of the values stands for the percentage of increase or decrease of the peak responses with respect to the corresponding uncontrolled response.

The case where the stiffness and strength degradation are considered shows the smaller reductions in any type of peak responses and in every value of the mass ratio, when it is compared to the case without infill wall.

It can also be seen that in the Case II in which the stiffness and strength degradation are considered, consisting in a more realistic scenario, the values of any of the peak responses for the mass ratio of 15% and 20% have only a slight variation, when comparing it with the other cases.

The same conclusions can be withdrawn when analyzing Table 3, considering now the peak responses of the system in study when subjected to the seismic acceleration, though the variation of the percentages of reduction between cases of hysteretic behavior and the values of mass ration are smaller due to the irregularity of the seismic acceleration.

Table 3 - Peak responses of the structure under the seismic acceleration of El Centro's earthquake.

Peak responses						
Case of Hysteretic behavior		**Mass ratio**	x (m)	ẋ (m/s)	ẍ (m/s^2)	drift (m)
Without infill wall		**0.05**	0.093 0.259	0.607 1.646	5.181 9.740	0.093 0.259
		0.10	0.086 0.189	0.592 1.123	5.007 6.977	0.086 0.184
		0.15	0.081 0.160	0.577 0.922	4.854 5.899	0.081 0.147
		0.20	0.077 0.141	0.562 0.779	4.798 5.108	0.077 0.132
With infill wall	**Case 0**	**0.05**	0.062 (-50%) 0.146 (-78%)	0.618 (2%) 0.895 (-84%)	6.264 (17%) 6.294 (-55%)	0.062 (-50%) 0.154 (-68%)
		0.10	0.059 (-45%) 0.118 (-60%)	0.613 (3%) 0.740 (-52%)	6.130 (18%) 5.617 (-24%)	0.059 (-45%) 0.124 (-48%)
		0.15	0.058 (-41%) 0.101 (-58%)	0.610 (5%) 0.643 (-43%)	6.007 (19%) 5.206 (-13%)	0.058 (-41%) 0.106 (-39%)
		0.20	0.056 (-38%) 0.090 (-56%)	0.608 (8%) 0.574 (-36%)	5.899 (19%) 4.888 (-5%)	0.056 (-38%) 0.094 (-40%)
	Case I	**0.05**	0.063 (-47%) 0.155 (-67%)	0.628 (3%) 0.930 (-77%)	6.247 (17%) 6.695 (-45%)	0.063 (-47%) 0.164 (-58%)
		0.10	0.061 (-41%) 0.125 (-50%)	0.623 (5%) 0.771 (-46%)	6.105 (18%) 5.636 (-24%)	0.061 (-41%) 0.132 (-39%)
		0.15	0.059 (-37%) 0.108 (-48%)	0.620 (7%) 0.669 (-38%)	5.975 (19%) 5.218 (-13%)	0.059 (-37%) 0.113 (-30%)
		0.20	0.058 (-34%) 0.096 (-46%)	0.618 (9%) 0.597 (-30%)	5.868 (18%) 4.894 (-4%)	0.058 (-34%) 0.101 (-31%)
	Case II	**0.05**	0.063 (-47%) 0.156 (-66%)	0.627 (3%) 0.931 (-77%)	6.221 (17%) 6.705 (-45%)	0.063 (-47%) 0.163 (-58%)
		0.10	0.061 (-41%) 0.126 (-49%)	0.622 (5%) 0.771 (-46%)	6.081 (18%) 5.613 (-24%)	0.061 (-41%) 0.132 (-40%)
		0.15	0.059 (-37%) 0.109 (-47%)	0.619 (7%) 0.669 (-38%)	5.952 (18%) 5.196 (-14%)	0.059 (-37%) 0.113 (-31%)
		0.20	0.058 (-34%) 0.097 (-45%)	0.617 (9%) 0.596 (-31%)	5.837 (18%) 4.872 (-5%)	0.058 (-34%) 0.100 (-32%)

a. The first and second lines represent the peak responses for the first and second floors, respectively, the main structure and the TMD.

b. The percentage on the left of the values stands for the percentage of increase or decrease of the peak responses with respect to the corresponding uncontrolled response.

Another different conclusion that can be seen in Table 3 is that the presence of the wall in the control performance of the TMD results in an increase of the peak responses in terms of velocities and accelerations of the structure, due to the constant irregularity verified along the seismic acceleration signal.

In each case of hysteretic behavior of the frame, as it moves on to a higher mass of the TMD the peak responses of the structure in terms of velocities and accelerations decreases, but when comparing it with the corresponding mass ratio of the case without infill wall it suffers an increase, although when considering the stiffness and strength degradation of the frame this increase is not very perceptive.

Observing now sequentially the graphs of Figures 4 to 7 considering the plain hysteretic behavior of the frame, its easily noticed the reduction of the response in terms of displacement with the increase of the TMD mass. The same happens when the system in study is subjected to the seismic acceleration. However it is not very perceptive.

When observing in sequence the graphs of the other hysteretic cases, for the two different acceleration signals, similar conclusions can be withdrawn. Nonetheless, in the hysteretic case where the stiffness and strength degradation are considered, the greater reduction is verified when comparing with the other hysteretic cases, yet the variation between the mass ratios of 15% and 20% is very small. Once more, in the scenario where the system in study is subjected to the seismic acceleration, there are significant reductions, although not very perceptive as the generic signal acceleration.

Analyzing the hysteretic loops now of the system subjected to the generic signal acceleration, considering the plain hysteretic behavior of the frame (Figure 8), where there is no strength degradation and stiffness degradation, in which the last one is defined by the same slope of the charge and discharge curves with the evolution of the hysteretic cycles, it can be seen in comparison with the uncontrolled case that as it moves on to a greater mass of the TMD the slimmer the hysteretic loops become, meaning that the displacements get smaller for the same strength capacity of the frame.

When considering the stiffness degradation (Figure 20), where the slope of the charge and discharge curves vary with the evolution of the hysteretic cycles, the same results are attained, i.e., with the increase of the mass ratio the slimmer the cycles become, noting a significant reduction of the displacement in relation with the uncontrolled case.

Observing now a more realistic hysteretic case, where the stiffness and strength degradation are considered together (Figure 33), it is evident the loss of strength capacity of the wall leading to greater displacements and eventually to a failure of the wall out of its plane, perceived by the permanent displacement in Figures 28 to 31 (green line), verified in the uncontrolled scenario. It was necessary to interrupt the simulation of the hysteretic loops for this case at *15,8s* since the wall failure resulted in a numerical instability.

It can be concluded that after the application of the vibration control system, the TMD, the reductions of the displacements for the same strength capacity of the frame are very significant. The mass ratio of 20% represents the best solution, though in most cases when comparing it with the solution of 15% the difference between them is not significant, when analyzing the hysteretic loops.

The same results can be seen when the system is subjected to the seismic acceleration, although the reductions are not so obvious as in the case with the generic signal acceleration, due to the irregularity of the acceleration.

REFERENCES

[1] Baber, T. T., & Noori, M. N. (1985). Article. Random Vibration of Degrading, Pinching Systems. J. Engrg. Mech., ASCE, 111(8), pp. 1010-1026.

[2] Bouc, R. (1967). Article. Forced Vibration of Mechanical Systems with Hysteresis. Proceedings 4th Conf. on Non-linear Oscillations.

[3] Braz-César M., Oliveira D., Barros R. (2013) Validação Numérica da Resposta Cíclica Experimental de Pórticos de Betão Armado (in portuguese). Revista da Associação Portuguesa de Análise Experimental de Tensões - Mecânica Experimental, 22, pp. 1-13.

[4] Casciati, F. (1989). Article. Stochastic Dynamics of Hysteretic Media. Amsterdam: Struct. Safety, 6, pp. 259-269.

[5] Folhento P., (2017) Estudo da Influência de Paredes de Alvenaria no Desempenho de Amortecedores de Massa Sintonizada. MSc Thesis, Politechnic Institute of Bragança.

[6] Paredes M., (2008) Utilização de Amortecedores de Massas Sintonizadas no Controlo de Vibrações em Estruturas. Faculty of Engineering of the University of Porto.

[7] Park, Y. J., Ang, A. H.-S., & Wen, Y. K. (1987). Article. Damage - Limiting Aseismic Design of Buildings. Earthquake Spectra, Vol. 3, Nº1.

[8] Reinhorn, A. M., Madan, A., Valles, R. E., Reinchmann, Y., & Mander, J. B. (1995). Technical Report NCEER-95-0018. Modeling of Masonry Infill Panels for Structural Analysis. State University of New York at Buffalo, Buffalo, N.Y.

[9] Sivaselvan, M. V., & Reinhorn, A. M. (2000). Article. Hysteretic Models for Deteriorating Ineslatic Structures. Journal of Engineering Mechanics, Vol. 126, Issue 6, pp. 633-640.

[10] Wen, Y.-K. (1976). Article. Method for Random Vibration of Vibration of Hysteretic Systems. J. Engrg. Mech. Div., ASCE, 102(2), pp. 249-263.